OPEN

5-Aminolevulinic Acid-derived Tumor Fluorescence: The Diagnostic Accuracy of Visible Fluorescence Qualities as Corroborated by Spectrometry and Histology and Postoperative Imaging

Walter Stummer, MD, PhD*
Jörg-Christian Tonn, MD, PhD‡
Claudia Goetz, MD, PhD§
Winfried Ullrich, MD¶
Herbert Stepp, PhD||
Andrea Bink, MD, PhD#
Thorsten Pietsch, MD, PhD**
Uwe Pichlmeier, PhD‡‡

*Department of Neurosurgery, University of Münster, Münster, Germany; ‡Department of Neurosurgery, Ludwig-Maximilians-University Munich, Klinikum Grosshadern, Munich, Germany; §Asklepios Klinik Nord Heidberg, Hamburg, Germany; ¶Department of Neurosurgery, University Regensburg Medical Center, Regensburg, Germany; ||Laser-Research Laboratory, LIFE-Center at University Hospital of Munich, Munich, Germany; #Department of Clinical Radiology, Universitätsklinikum Münster, Münster, Germany; **Department of Neuropathology, Universtitätsklinikum Bonn, University of Bonn Medical Center, Bonn, Germany; ‡‡Medac, Gesellschaft für klinische Spezialpräparate mbH, Wedel, Germany

Correspondence:
Walter Stummer, MD, PhD,
Neurochirurgische Klinik,
Universitätsklinikum Münster,
Albert-Schweitzer-Campus 1,
Gebäude A1, 48149 Münster,
Germany.
E-mail: Walter.Stummer@ukmuenster.de

Received, August 15, 2013.
Accepted, November 25, 2013.
Published Online, December 12, 2013.

BACKGROUND: 5-Aminolevulinic acid is used for fluorescence-guided resections. During resection, different macroscopic fluorescence qualities ("strong," "weak") can be distinguished that help guide resections.

OBJECTIVE: This prospective study was designed to assess the reliability of visible fluorescence qualities by spectrometry, pathology, and imaging.

METHODS: Thirty-three patients with malignant gliomas received 5-aminolevulinic acid (20 mg/kg). After debulking surgery, standardized biopsies were obtained from tissues with "weak" and "strong" fluorescence and from nonfluorescing near and distant brain for blinded assessment of cell density and tissue type (necrosis, solid or infiltrating tumor, normal tissue). The positive predictive value was calculated. Unresected fluorescing tissue was navigated for blinded correlation to postoperative magnetic resonance imaging (MRI). Receiver operating characteristic curves were generated for assessing the classification efficiency of spectrometry.

RESULTS: "Strong" fluorescence corresponded to greater spectrometric fluorescence, solidly proliferating tumor, and high cell densities, whereas "weak" fluorescence corresponded to lower spectrometric fluorescence, infiltrating tumor, and medium cell densities. The positive predictive value was 100% in strongly fluorescing tissue and 95% in weakly fluorescing tissue. Spectrometric fluorescence was detected in marginal tissue without macroscopic fluorescence. Depending on the threshold, spectrometry displayed greater sensitivity but lower specificity (accuracy 88.4%). Residual MRI enhancement in the tumor bed was detected in 15 of 23 (65%) patients with residual fluorescence, but in none of the patients without residual fluorescence.

CONCLUSION: Macroscopic fluorescence qualities predict solid and infiltrating tumor, providing useful information during resection. Fluorescence appears superior to contrast enhancement on MRI for indicating residual tumor. Spectrometry, on the other hand, is more sensitive but less specific, depending on threshold definition.

KEY WORDS: 5-Aminolevulinic acid, Fluorescence-guided resection, Malignant glioma, Sensitivity, Specificity, Spectrometry

Neurosurgery 74:310–320, 2014 DOI: 10.1227/NEU.0000000000000267 www.neurosurgery-online.com

ABBREVIATIONS: 5-ALA, 5-aminolevulinic acid; **CI,** confidence interval; **gamma-GT,** gamma-glutamyl transpeptidase; **GBM,** glioblastoma multiforme; **NPV,** negative predictive value; **PPIX,** protoporphyrin IX; **PPV,** positive predictive value; **SD,** standard deviation; **WHO,** World Health Organization

5-Aminolevulinic acid (5-ALA) elicits synthesis and accumulation of fluorescing porphyrins, predominantly protoporphyrin IX (PPIX), in malignant glioma tissue and is being used for their intraoperative identification.[1-13]

This fluorescence can be made visible macroscopically with the aid of standard surgical microscopes

equipped with optical filters[1,4,6,9,14-16] and is highly predictive of malignant glioma tissue.[1,9,11,13,17,18]

The lack of visible fluorescence in adjacent tissue, however, is not highly predictive of normal tissue, because biopsies taken from these areas have frequently been infiltrated by tumor cells, corresponding to a low negative predictive value.[1,6,9,18] Nonvisual methods such as high-resolution spectrometry[11,13] allow PPIX to be detected with greater sensitivity in these regions.

Regarding visible fluorescence, 2 types have been described,[1,3,9,17] "solid," "red," or "strong" and "weak," "vague," or "salmon" fluorescence (Figure 1A, B). Solidly proliferating, central, viable tumor with vascular proliferation has been associated with intense red fluorescence, and surrounding infiltrating tumor with moderate to high cell density has been associated with pink fluorescence.[9,11,17] This information may help guide surgery macroscopically because the resection of strongly fluorescing tissue, which signifies gross tumor, may have a significant influence on short-term prognosis, whereas resections of weakly fluorescing tissue, which signifies infiltrating tissue, may be close to or involved with the functional brain.[9]

To corroborate the value and reliability of macroscopic, ie, visible, fluorescence qualities for guiding surgery, we have performed a systematic collection of biopsies with differing visible fluorescence qualities, analyzed by in situ spectrometry and neuropathology. Also, we have used neuronavigation to correlate residual fluorescence with the occurrence and the volume of contrast-enhancing tumor on early postoperative magnetic resonance imaging (MRI). For bias reduction, we have included 4 different centers with blinded neuropathological and neuroradiological assessments.

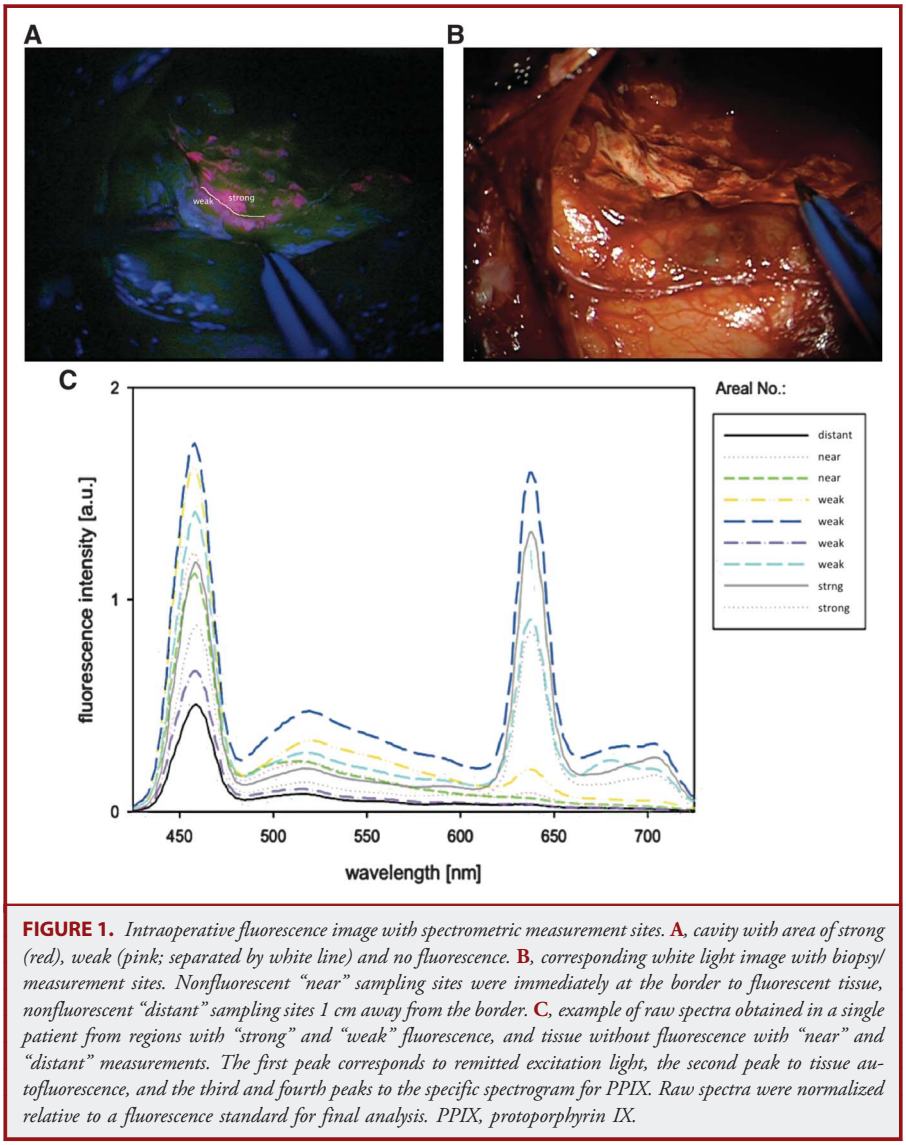

FIGURE 1. *Intraoperative fluorescence image with spectrometric measurement sites.* **A**, *cavity with area of strong (red), weak (pink; separated by white line) and no fluorescence.* **B**, *corresponding white light image with biopsy/measurement sites. Nonfluorescent "near" sampling sites were immediately at the border to fluorescent tissue, nonfluorescent "distant" sampling sites 1 cm away from the border.* **C**, *example of raw spectra obtained in a single patient from regions with "strong" and "weak" fluorescence, and tissue without fluorescence with "near" and "distant" measurements. The first peak corresponds to remitted excitation light, the second peak to tissue autofluorescence, and the third and fourth peaks to the specific spectrogram for PPIX. Raw spectra were normalized relative to a fluorescence standard for final analysis. PPIX, protoporphyrin IX.*

PATIENTS AND METHODS

Our protocol was approved by the Independent Ethics Committee of the University of Munich, Project-No. 201/02 and sponsored by Medac, Wedel, Germany.

Eligibility Criteria

In this prospective study, patients aged 18 to 75 years with a Karnofsky Performance Scale of ≥60, an MRI suggesting malignant glioma (World Health Organization [WHO] grades III-IV), first diagnosis of tumor, without tumor-specific pretreatments, and with intended surgery were considered eligible. Patients in whom safe gross total resections were not considered possible were preferred. Patients with porphyria, hypersensitivity to porphyrins, renal or hepatic insufficiency, or other malignancies (with the exception of basaliomas) were to be excluded from the study. Gamma-glutamyl transpeptidase (gamma-GT) was required to be lower than 100 U/L.

Study Objectives

The primary objective and the basis for biometry was to determine the positive predictive value (PPV) of visible fluorescence in a patient-based analysis, ie, the percentage of patients showing tumor in all biopsies with fluorescence. For sensitivity analyses, PPV was also calculated for pooled biopsies from all patients as the percentage of biopsies with tumor cells among all fluorescing biopsies, either with weak or strong fluorescence.

The secondary aims were as follows:

1. To correlate visible fluorescence qualities ("weak," "strong") with spectrometry, tumor cell density, and tissue morphology (viable, solidly proliferating tumor, infiltrating tumor, necrosis, normal brain tissue).
2. To correlate spectrometric fluorescence in tissues without visible fluorescence with tumor cell density and morphology. Samples were taken immediately adjacent to fluorescing tumor regions ("near") as well as from nonfluorescing regions 1 cm away from fluorescing tissue ("distant").
3. To correlate the location of residual visible fluorescence determined by neuronavigation to early postoperative MRI (within 72 hours after surgery). If tumor was knowingly left unresected, the surgeon recorded whether tumor was suspected under fluorescence conditions only (WL− and FL+), or both under fluorescence and standard white light conditions (WL+ and FL+), or under white light only (WL+ and FL−). The visible *area* of residual tumor was quantified. Screenshots from neuronavigation were collected for comparison with postoperative MRI.

Intraoperative Procedures

Patients were pretreated with 3 × 4 mg dexamethasone daily for at least 2 days and until postoperative MRI had been obtained. 5-ALA (20 mg/kg body weight; medac, Wedel, Germany) was administered in 50 mL of water 3 hours before anesthesia. Patients were protected from direct sunlight before surgery and maintained in subdued light until the following morning.

The Brainlab Vector Vision system was used for navigation and the Zeiss OPMI Neuro FL NC4 microscope for surgery in all 4 centers.

After craniotomy, the tumor was exposed and resected up to its fluorescing margins. The surgeon then selected 3 regions of interest with strong fluorescence. For each region, spectrometry was performed with biopsy thereafter. The same procedure was applied for 3 regions with weak fluorescence, if weak fluorescence could be identified. Next, 2 tissue regions without visible fluorescence immediately outside the boundary of fluorescing tissue were selected ("near" brain), as well as 2 regions at a distance of 1 cm from the adjacent brain ("distant" brain; Figure 1) for spectrometry and biopsy (Figure 1), if biopsy was possible safely, for instance, in tissues from the approach corridor.

At the end of surgery, the surgeon recorded any areas of residual fluorescence left unresected by using neuronavigation for comparison with MRI, assessed their fluorescence quality, and estimated their size.

Spectrometry

Spectrometry was performed with the D-Light System (Karl Storz, Tuttlingen, Germany) coupled to a fiber probe array consisting of a centrally arranged 400-μm detection fiber surrounded by six 400-μm excitation fibers, and to a S2000 spectrometer (Ocean Optics, Eerbeek, Netherlands). Reflected excitation light was filtered by a longpass filter (440 nm) to block most of the light (with the exception of a small residual remission peak at 456 nm). Three spectra were obtained at each measurement site and averaged (Figure 1C). All spectra were normalized relative to the peak intensity of a fluorescing, nonbleaching reference (commercially available red rubber eraser) fluorescing in the range of the porphyrin spectrum acquired before each tissue measurement to account for short-term fluctuations in excitation light.

PPIX exhibits characteristic fluorescence peaks at 635 nm, which is in the visible red, and a lower peak at 704 nm; the peak at 704 nm is in the near infrared and not clearly visible to the eye. Therefore, the 635-nm peak was used for quantifying fluorescence. This peak corresponds to the visual impression of the brightness in the red wavelength, comprising autofluorescence, PpIX fluorescence, and tissue absorption.

Postoperative Assessments

Screenshots from neuronavigation were compared with early postoperative MRI by blinded reference neuroradiologists (Institute for Neuroradiology, University of Frankfurt). The cutoff for residual tumor enhancement was defined as 1 voxel or 0.175 cm.[2,8,10] Residual contrast-enhancing tumor volume was calculated by segmentation.

Tumors were graded by blinded neuropathologists (Department of Neuropathology, University of Düsseldorf) according to the WHO grading system with respect to tumor type and grade with the use of hematoxylin and eosin and reticulin staining. Tumor cellularity was assessed per biopsy by the use of a simple semiquantitative scale discerning 5 categories: 0%, 1% to 25%, 26% to 50%, 51% to 75%, and 76% to 100%. For all statistical calculations, the average values of these categories were applied, ie, 0%, 13%, 38%, 63%, and 88%. In addition, the gross morphology of tissue was assessed in 4 classes, ie, solidly proliferating tumor (no intervening brain tissue), infiltrating tumor, necrosis, or normal brain tissue.

In areas with ambivalent tumor tissue infiltration, immunohistochemistry, including glial fibrillary acidic protein, MIB-1 (Ki-67), and p53, staining was performed for unequivocally identifying infiltrating tumor cells (Figure 2). In individual cases, additional staining was performed for MAP-2, Lu-5, CD45, CD20, CD68, and CD34. All assessments of tissue type and cell density were performed separately by 2 board-certified neuropathologists. Disagreements between the neuropathologists were resolved by professional discussion.

Statistical Methods

Sample Size

Thirty-three patients were required to calculate PPV with a precision of ±20% expressed as the half-length of the associated 2-sided 90%

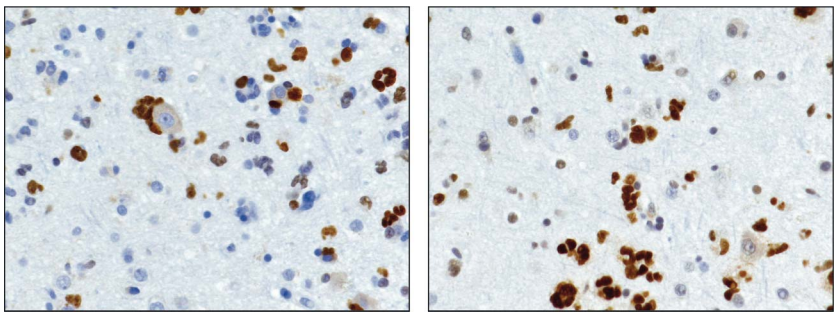

FIGURE 2. *Infiltrating tumor regions with low cell density. Immunohistochemistry was used for unequivocal identification of tumor cells.* **Left**, *MIB-1 (Ki-67) staining.* **Right**, *p53 staining.*

confidence interval (CI) with a power of 80%, assuming the expected PPV to be 90%.

Biometric Analysis

Exact 90% Clopper-Pearson confidence intervals were applied for estimating PPVs on a patient-based level. Analyses were also stratified by fluorescence qualities. PPVs were analogously analyzed from pooled biopsies.

The mean values of all spectrometric measurement within each fluorescence quality as well as corresponding tumor cell densities per measurement site were averaged within each patient. The resulting averages were used for correlations with fluorescence quality.

Friedman tests were applied for exploring global homogeneity between fluorescence qualities followed by Wilcoxon signed-rank sum tests for pairwise comparisons. Nonparametric Kruskal-Wallis tests served for assessing global homogeneity between fluorescence qualities, followed by pairwise Wilcoxon-Mann-Whitney tests.

RESULTS

Thirty-nine patients were recruited, of which 6 had to be excluded (2 with metastases, 2 with a gamma-GT >100 U/L, and 2 patients not operated on for anesthesiological reasons). Thirty-three patients with malignant gliomas (29 glioblastomas, 4 anaplastic astrocytomas) were examined according to protocol (Table 1).

Positive and Negative Predictive Values

In the patient-based analysis, false-positive fluorescence was observed in 7 samples (from 5 of 33 patients), all from regions with weak fluorescence. Thus, the patient-based PPV was 84.8% (90% CI, 70.7%-93.8%). For glioblastomas only, the patient-based PPV was 82.8% (67.1%-93%). No false-positive samples were found in patients diagnosed with anaplastic gliomas (WHO grade III).

When biopsies were pooled, the overall PPV of fluorescence was 96.2% (90% CI, 93.0%-98.2%), for strong fluorescence the overall PPV was 100% (96.9%-100.0%), and for "weak" fluorescence the overall PPV was 92.2% (85.9%-96.3%). For glioblastomas only, the overall PPV of fluorescence was 95.7% (91.1%-98%), for strong fluorescence the overall PPV was 100% (96.6%-100%), and for weak fluorescence the overall PPV was 91% (83.8%-95.7%).

The negative predictive value (ie, the number of nonfluorescing biopsies without tumor) was 45 among 114 nonfluorescing samples, ie, 39.5%. For glioblastomas only, this value was 40% (40 among 100 nonfluorescing biopsies).

Correlation Between Visible Fluorescence, Spectrometry, and Histology

Spectrometric fluorescence was measured at 318 locations. In 18 of these locations, all of which did not show fluorescence and all were distant from fluorescing tissue, investigators did not collect

TABLE 1. Demographic Data (n = 33)[a]

Age	
Median (range)	61.0 (21-72)
Mean (SD)	56.6 (13.4)
KPS	
Median (range)	90 (70-100)
70	5 (15.2%)
80	9 (27.3%)
90	11 (33.3%)
100	8 (24.2%)
Histology	
Anaplastic astrocytoma (grade III)	4 (12.1%)
Glioblastoma (grade IV)	29 (87.9%)
Location	
Hemisphere	
Right	18 (54.5%)
Left	15 (45.5%)
Frontal	4 (12.1%)
Occipital	2 (6.1%)
Parietal	17 (51.5%)
Temporal	17 (51.5%)
Ventricular involvement	22 (66.7%)
Multilocular	2 (6.1%)
Tumor volume, cm^3	
Median (range)	36.6 (1-169.9)
Mean (SD)	42.6 (33.3)

[a]KPS, Karnofsky Performance Scale; SD, standard deviation.

biopsies to avoid harming healthy brain. Thus, 300 biopsies were collected for histological assessments.

Macroscopically, tissues with "weak" fluorescence always bordered distally to tissues with "strong" fluorescence.

Spectrometric fluorescence was highest in tissue with "strong" visible fluorescence and less in tissues with "weak" fluorescence (Figure 3). Notably, spectrometric fluorescence was detected in samples outside visible fluorescing tissue and was significantly higher in "near" than in "distant" samples.

Cell density was higher in regions with "strong" fluorescence in comparison with regions with "weak" fluorescence (Figure 4), but tumor cells were also found in tissues without visible fluorescence. All differences in cell densities, when stratified by the fluorescence type, were significant, with the exception of a marginal difference ($P = .07$) between biopsies taken from "near" and "distant" regions.

As demonstrated in Figure 5, "strong" fluorescence corresponded mainly to solidly proliferating tumor and "weak" fluorescence corresponded mainly to infiltrating tumor. "Near" and "distant" tissues without visible fluorescence showed mostly infiltrating cells or no tumor. Infiltrating tumor was more commonly found in "near" samples.

For further information on how reliably the visual fluorescence qualities "strong" and "weak" predict spectrometric fluorescence intensities and tumor cell density on a patient-to-patient basis, we plotted spectrometric fluorescence against cell density and stratified by the visual fluorescence impression (Figure 6). For this purpose, multiple measurements within the same fluorescence quality in 1 patient were averaged. "Strong" visual fluorescence in individual samples was related to high cell densities and strong fluorescence, whereas samples designated as "weak" by study surgeons had low cell densities and low spectrometric fluorescence. Overlap between these categories was minimal.

No meaningful differences were found between patients with glioblastomas in comparison with patients with anaplastic gliomas (WHO grade III; individual data not shown).

Spectrometric Discrimination of Tumor Depending on Preset Threshold

When considering spectrometric fluorescence as a diagnostic tool for discrimination of infiltrated brain, it can be expected that the *threshold* chosen for discrimination will directly influence sensitivity and specificity. For this reason, receiver operating characteristic curves[19] were calculated from all data that illustrated the relationship between discrimination threshold, sensitivity, and specificity (Figure 7). The area under the curve, a measure for the accuracy, was 88.4%. Choosing, eg, a spectrometric threshold of 0.28 a.u. would result in a specificity of about 95% with a sensitivity of 72%. On the other hand, selecting a lower threshold, eg, 0.08, would increase sensitivity to 94% at the cost of specificity, which would be 41%.

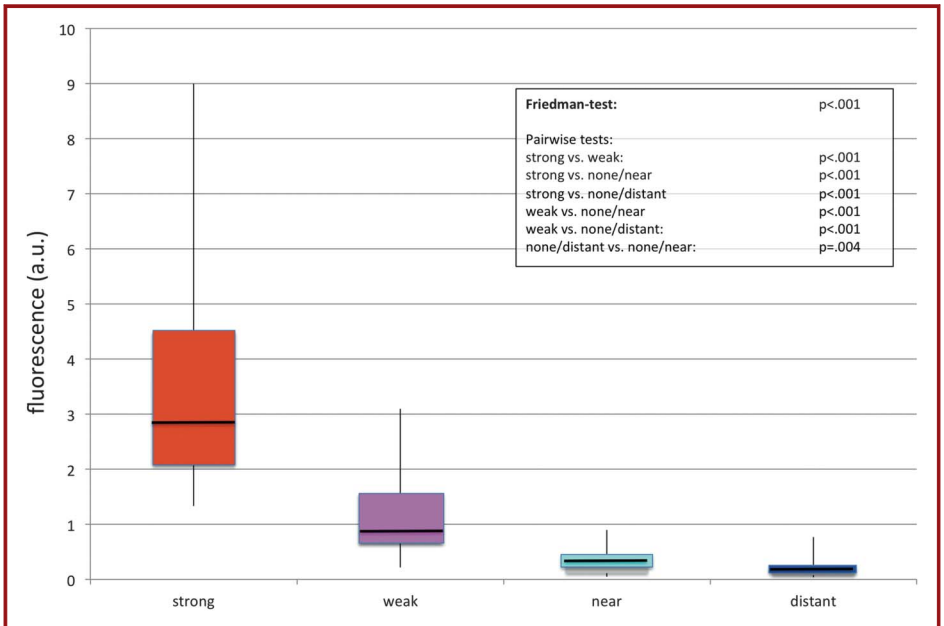

FIGURE 3. *Relationship between visual (macroscopic) fluorescence and spectrometric fluorescence. Multiple measurements for fluorescence in single patients at comparable locations were averaged for this analysis. These values are stratified by individual fluorescence qualities as perceived visually through the surgical microscope ("strong," n = 96; "weak," n = 90) or nonfluorescing adjacent tissue ("near," n = 66; "distant," n = 66). Boxes signify medians, 25th and 75th percentiles; whiskers signify ranges.*

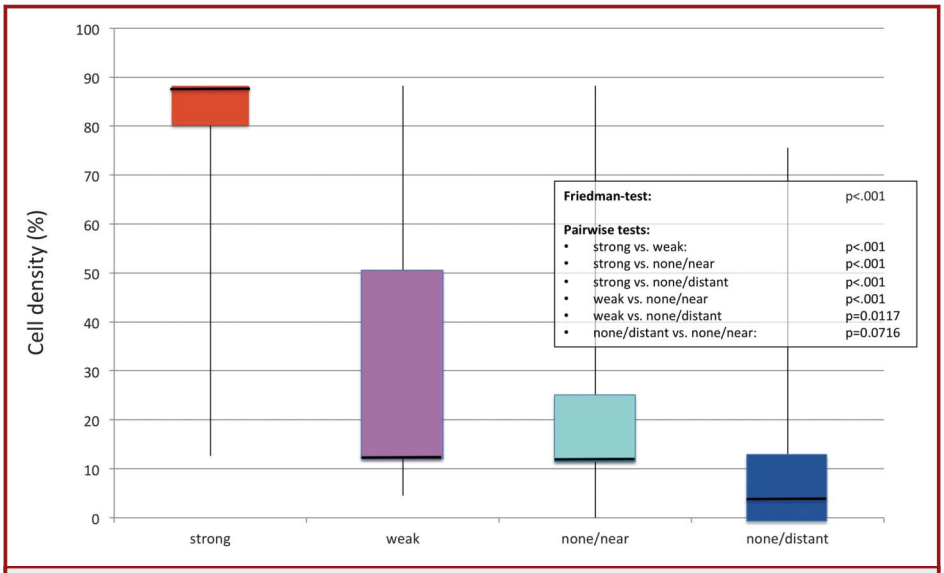

FIGURE 4. *Relationship between visual (macroscopic) fluorescence and cell densities. Multiple measurements for fluorescence in single patients at comparable locations were averaged for this analysis. These values are stratified by individual fluorescence qualities as perceived visually through the surgical microscope ("strong," n = 96; "weak," n = 90) or nonfluorescing adjacent tissue ("near," n = 66; "distant," n = 48). Boxes signify medians, 25th and 75th percentiles; whiskers signify ranges.*

Correlation Between Residual Fluorescence and Postoperative MRI

Fluorescing tissue was knowingly left unresected in 23 (69.7%) cases (glioblastoma multiforme [GBM] only, 70.0%). In merely 15 (65.2%) of these, enhancement was found on early MRI (GBM only, 63.0%). In 2 of 10 patients without residual fluorescence (20%), radiologists detected residual tumor on postoperative MRI, which corresponded to a second tumor at a distance from

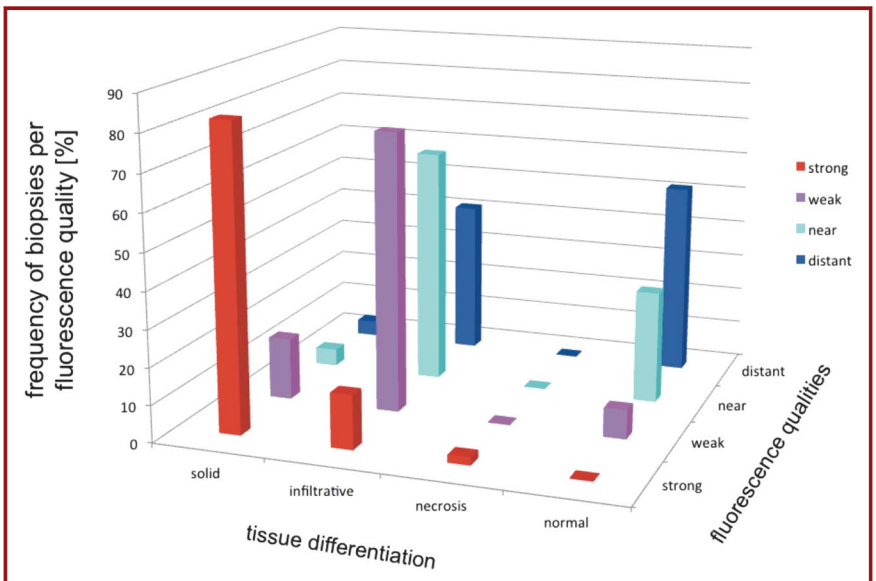

FIGURE 5. *Tissue differentiation stratified by visible fluorescence qualities and frequency of biopsies obtained per fluorescence quality ("strong," n = 96; "weak," n = 90) or nonfluorescing adjacent tissue ("near," n = 66; "distant," n = 48). The ordinate gives the percentage of biopsies from a given fluorescence quality with a particular tissue morphology.*

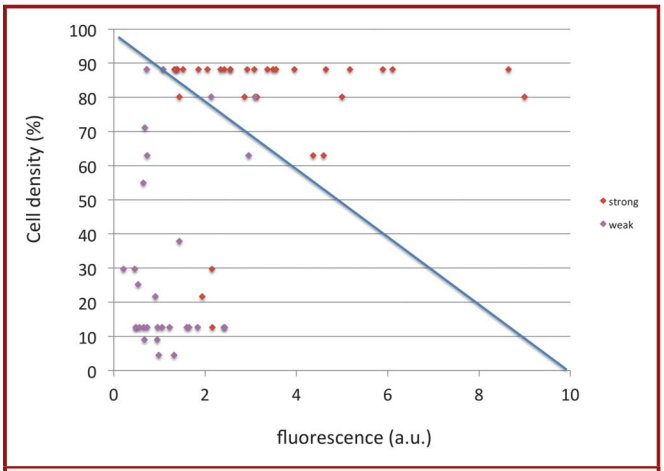

FIGURE 6. *In order to compare the results from different patients operated on by different surgeons at different sites regarding the reproducibility of results, this graph relates spectrometric fluorescence to histological cell densities stratified by fluorescence quality ("strong," "weak"). For this graph, all measurements obtained from the same fluorescence quality in a single patient were averaged (n = 33). "Strong" visual fluorescence was related to high cell densities and strong spectrometric fluorescence, whereas "weak" fluorescence was related to lower cell densities and low spectrometric fluorescence. There was little overlap.*

the operated tumor with intervening, nonenhancing brain. Both were patients with glioblastoma. One postoperative MRI could not be evaluated because of image distortions by movement; and, in 1 patient with cerebral infarction, no MRI was performed.

Residual fluorescence was documented in 42 regions by screenshots from neuronavigation (GBM only, 39 regions). Ten of these regions (23.8%) were also identified under white light (GBM only, 8 regions, 22.2%). In 1 patient with glioblastoma, a rather large residual tumor of greater than 50 cm^3 was not detected under white light, but only by the use of fluorescence. In

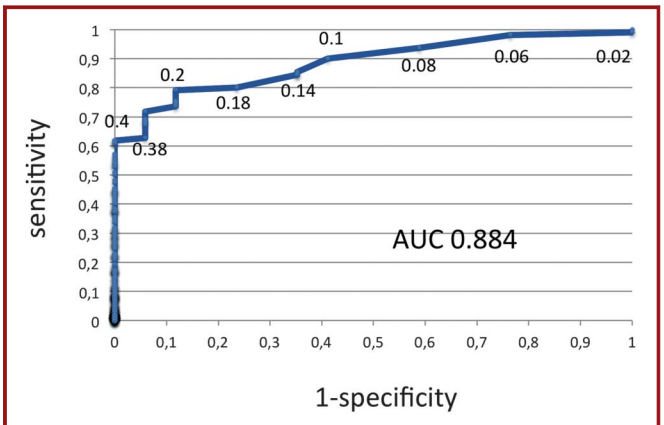

FIGURE 7. *Receiver operating characteristic (ROC) curves for assessing the classification efficiency of spectrometry. The area under the curve (AUC) was 0.88. Threshold values are indicated in the curve for resulting specificities and sensitivities.*

no case was tumor identified under white light alone that did not fluoresce (Table 2).

Fluorescing area and type of fluorescence predicted the volume of residual tumor on MRI. Large fluorescing areas (>3 cm^2) corresponded to large residual volumes (27.3 ± 37.4 cm^3, mean ± standard deviation [SD]). Smaller areas of 1 to 3 cm^3 and <1 cm^3 corresponded to smaller residual volumes of 11.1 (SD 14.6) cm^3 and 1.2 (SD 1.5) cm^3, respectively. In most cases, the areas that were left unresected were categorized as "small."

Locations of residual fluorescence perceived as "strong" corresponded to a residual volume of 37.6 (SD 22.9) cm^3. Regions with "weak" fluorescence corresponded to a volume of 1.1 (SD 1.3) cm^3. The type of fluorescence in those areas left unresected was mostly characterized as "weak."

Safety Results

Two patients died perioperatively, one owing to bihemispheric infarction of undetermined cause (autopsy was refused), and the other owing to aspiration pneumonia. Deaths were not considered as being related to 5-ALA. Serious adverse events were reported in 22.2% of 36 patients having received ALA (3 convulsions, 2 aphasias, 1 hemiparesis, 2 cerebral infarctions, 1 aspiration pneumonia, 1 wound infection, 1 hypotension). All serious adverse events resolved with the exception of 2 perioperative deaths. A transient elevation of transaminases (alanine aminotransferase/glutamic-pyruvate transaminase in 68.6% and aspartate aminotransferase/glutamic oxaloacetic transaminase in 44.4% of patients), gamma-GT (in 65.7% of patients), and amylase (in 36.1% of patients) between 1 and 14 days after surgery was observed.

DISCUSSION

5-ALA has gained regulatory approval in Europe based on the data from a randomized study[11] and is now widely used. Intraoperative discrimination of fluorescing porphyrins induced in tissue is purely visual with the use of adapted surgical microscopes. No additional technology is required, allowing real-time resection of tumor by simply switching illumination modes, making its usage simple and straightforward.

Fluorescence may also be detected nonvisually by using spectrometry with greater sensitivity beyond what is visible by using the surgical microscope.[11,13] On the other hand, spectrometry allows only very local assessments of fluorescence and does not provide the general overview of the resection cavity obtained with the microscope. It is unclear how visual and spectrometric fluorescence compare in glioma surgery.

The present analysis aims at corroborating the value of the visual fluoresce qualities "strong" and "weak" in predicting tissue morphology and spectrometric fluorescence.

Positive Predictive Value of Fluorescence

We found a high PPV of 96% of 5-ALA-derived fluorescence for identifying tumor, corroborating earlier findings.[1,3,6,9,17,18] Falsely fluorescing biopsies were exclusively from areas perceived

TABLE 2. Relationship Between Intraoperative Tumor and Postoperative MRI[a]

Intraoperative Assessment	Residual Tumor Postoperative MRI					
			Volume of Residual Tumor, cm^3			
	Fluorescing Tumor Regions, n (%)	Regions With Enhancement, n (%)	Min	Median	Max	Mean	SD
Total number of regions	42 (100)	14 (33.3)	0.19	0.89	53.76	6.76	15.23
WL+ and FL+	10 (23.8)	4 (40)	0.35	0.89	2.32	1.19	1.02
WL+ and FL−	0	0	0	0	0	0	0
WL− and FL+	32 (76.2)	10 (31.3)	0.19	0.83	53.76	8.43	17.19
Area of residual fluorescence (WL−, FL+)							
Small (<1 cm^2)	23 (71.9)	6 (26.1)	0.19	0.45	3.7	1.24	1.48
Medium (1-3 cm^2)	7 (21.9)	2 (28.6)	0.73	11.09	21.4	11.1	14.6
Large (>3 cm^2)	2 (6.3)	2 (100)	0.92	27.34	53.76	27.34	37.36
Quality of fluorescence (WL−, FL+)							
Strong	5 (25.6)	2 (40.0)	21.4	37.6	53.8	37.6	22.85
Weak	27 (84.4)	8 (29.6)	0.19	0.61	3.7	1.14	1.27

[a]WL+, identifiable under white light; FL+, fluorescing; WL−, not detectable under white light; FL−, no fluorescence; SD, standard deviation.

as "weak" by surgeons, that is, from tissue regions intimately associated with the tumor margin and not from remote parts of the brain. These samples were only found in patients with glioblastoma. All samples perceived to have strong fluorescence correctly predicted tumor.

Falsely fluorescing samples have also been described by others.[6,9,20,21] Among 86 fluorescence-positive biopsies, Roberts et al[6] recorded 4 biopsies without tumor. Three of these biopsies were either necrotic or showed prominent vasculature. Only 1 sample appeared normal. Utsuki et al[21] found 1 falsely positive sample in primarily diagnosed malignant gliomas. This sample was strongly infiltrated by granulocytes and was clearly abnormal histologically. The numbers of falsely labeled tissue may be higher in recurrences where reactive astrocytes are thought to play a role; other explanations concern leakage of PPIX into surrounding edema, the latter on a microscopic level.[3,20,21]

In the present study, we did not focus on the microscopic distribution of PPIX fluorescence. Rather, the analysis of fluorescing tissues was based on standard neuropathological criteria. Therefore, our results do not prove the cellular specificity of 5-ALA and resultant PPIX fluorescence, ie, whether fluorescence was exclusively located in the intracellular space of malignant cells even in those samples in which macroscopic fluorescence was related to tumor. Reactive astrocytes or inflammation may have contributed to the fluorescence signal perceived in such samples. Overall, however, the present observations confirm that the surgical microscope will indicate tumor or tumor-infiltrated brain to an extent that can be well relied upon for guiding macroscopic resection.

Conversely, the negative predictive value (NPV) using our biopsy algorithm was not high, ie, 40%, and similar to another study,[6] whereas another study found a higher NPV of 66%.[1] In contradistinction to the PPV, the NPV depends on how nonfluorescing biopsies are collected. If sampling sites are remote to the tumor, the likelihood of not finding tumor cells will be higher than if biopsies are collected close to the tumor. Nevertheless, despite these limitations in sensitivity, fluorescence detects tumor beyond tissues with contrast enhancement on MRI, as our present data and the data of others have shown,[4,6,9] and contrast-enhancing tumor is generally considered the surgical target.[22-25]

Some investigators[6,11,13,17] have formally calculated diagnostic sensitivity and specificity to reach similar conclusions as ours. As with the NPV, these measures depended greatly on the sampling algorithm of nonfluorescing tissue. Because investigators do not appear to use comparable biopsy algorithms, their results cannot simply be compared. For these reasons, we chose to primarily calculate the PPV for quantifying the usefulness of fluorescence.

Reliability of Visual Fluorescence Qualities for Discriminating Tumor Tissue Subtypes

The central aim of our analysis was to objectively determine the value of visible fluorescence qualities "strong" and "weak"[3,6,17] for predicting tissue morphology. To reduce bias, 4 neurosurgical centers were involved. Additionally, neuropathologists and neuroradiologists were blinded to the intraoperative findings.

Our study demonstrated macroscopic, ie, visible, fluorescence to be very significantly related to spectrometric fluorescence. Biopsies from strongly fluorescing tissues contained mostly high-density, solidly proliferating tumor; biopsies taken from weakly fluorescing tissue contained mostly infiltrating tumor with low to medium cell density.

Unfortunately, our study was not designed to investigate interobserver reliability for the discrimination of tissue morphology by visual fluorescence qualities. This would have required at least 2 study surgeons independently rating the same sample. However, we were able to demonstrate that, when results obtained for fluorescing samples are compared on a patient-to-patient basis, the discrimination between samples rated as displaying "strong" fluorescence and samples rated as showing "weak" fluorescence

remained good, even though patients were operated on at different sites by different surgeons. "Strong" fluorescence was related to high cell densities or strong spectrometric fluorescence, whereas "weak" fluorescence was generally related to low spectrometric fluorescence or low cell densities.

Thus, we conclude that macroscopic fluorescence qualities can be relied on for guiding the surgeon's decisions regarding resection, allowing macroscopic identification of the infiltrating tumor.

Spectrometry

Spectrometry is a nonvisual tool for assessing tissue fluorescence.[26-29] Spectrometric fluorescence extended beyond visible fluorescence in the present study and may help in identifying more tumor. This has been pointed out previously.[11,13,30-33]

One focus of our study was to relate spectrometric data to the visible red fluorescence. The spectrometric values were determined as the intensity of peak fluorescence of the PPIX at 635 nm, a composite of PPIX fluorescence, autofluorescence, and absorption, which approximates the visual impression. Valdés et al[13] used a different algorithm to overcome effects of heterogeneous optical tissue properties (light absorption and scattering) and illumination geometry. Their values correspond more closely to the actual tissue concentration of PPIX. In their calculation of apparent sensitivity and specificity, the visual impression resulted in a specificity of 100% and a sensitivity of 47%. Spectrometry allowed sensitivity to be increased to 84% while reducing specificity to 92%. These values, however, were generated in 14 patients with various histologies (2 low-grade gliomas, 6 meningiomas, and 3 metastasis), but only in 3 high-grade gliomas. Our study provides data on a larger cohort of patients with malignant glioma. The area under the receiver operating characteristic curve as indicator of classification efficiency was 87% in the series by Valdés et al[13] In our analysis, we found a similar value of 88% even though the methodology differed, which appears reassuring.

MRI and Fluorescence

The present analysis indicates a relationship, in particular, of solid fluorescence and enhancement on early postoperative MRI. In an initial investigation of 11 patients by the use of neuronavigation, Roberts et al[6] showed that visible fluorescence corresponds to enhancing tumor. We now demonstrate in a larger cohort that visible fluorescence extends beyond contrast enhancement on MRI and that fluorescence area and quality were predictive of residual contrast-enhancing tumor volumes. Thus, the surgeon, if faced with large areas of residual fluorescence or strong fluorescence, will be advised to continue resection if safely possible.

CONCLUSION

Our investigation confirms the high PPV of macroscopically visible, ALA-derived fluorescence in malignant gliomas for identifying residual tumor beyond enhancing regions on MRI. Sensitivity is increased by spectrometry, albeit with less specificity. Importantly, subjectively perceived fluorescence qualities "strong" and "weak" correlate highly with spectrometric fluorescence, cell density, and tissue differentiation (solidly proliferating, infiltrating) and predict tumor tissue morphology as a guide for the extent of resection, for instance, warning the surgeon that he is in infiltrating tumor when "weak" fluorescence is encountered. In addition, residual fluorescence was correlated with residual tumor on MRI, giving the surgeon useful information intraoperatively.

Disclosures

This study was supported by medac, Gesellschaft für klinische Spezialpräparate mbH, Wedel. Dr Pichlmeier is biometrician affiliated with this company. Dr Stummer has received lecture and consultant fees from medac. Otherwise, the authors have no personal, financial, or institutional interest in any of the drugs, materials, or devices described in this article.

REFERENCES

1. Díez Valle R, Tejada Solis S, Idoate Gastearena MA, García de Eulate R, Domínguez Echávarri P, AristuMendiroz J. Surgery guided by 5-aminolevulinic fluorescence in glioblastoma: volumetric analysis of extent of resection in single-center experience. *J Neurooncol.* 2011;102(1):105-113.
2. Floeth FW, Stummer W. The value of metabolic imaging in diagnosis and resection of cerebral gliomas. *Nat ClinPract Neurol.* 2005;1(2):62-63.
3. Nabavi A, Thurm H, Zountsas B, et al. Five-aminolevulinic acid for fluorescence-guided resection of recurrent malignant gliomas: a phase ii study. *Neurosurgery.* 2009;65:1070-1077.
4. Aldave G, Tejada S, Pay E, et al. Prognostic value of residual fluorescent tissue in glioblastoma patients after gross total resection in 5-aminolevulinic Acid-guided surgery. *Neurosurgery.* 2013;72:915-920.
5. Pichlmeier U, Bink A, Schackert G, Stummer W. Resection and survival in glioblastoma multiforme: an RTOG recursive partitioning analysis of ALA study patients. *Neuro Oncol.* 2008;10(6):1025-1034.
6. Roberts DW, Valdes PA, Harris BT, et al. Coregistered fluorescence-enhanced tumor resection of malignant glioma: relationships between δ- aminolevulinic acid-induced protoporphyrin IX fluorescence, magnetic resonance imaging enhancement, and neuropathological parameters. Clinical article. *J Neurosurg.* 2011;114(3):595-603.
7. Roessler K, Becherer A, Donat M, Cejna M, Zachenhofer I. Intraoperative tissue fluorescence using 5-aminolevolinic acid (5-ALA) is more sensitive than contrast MRI or amino acid positron emission tomography ((18)F-FET PET) in glioblastoma surgery. *Neurol Res.* 2012;34(3):314-317.
8. Schucht P, Beck J, Abu-Isa J, et al. Gross total resection rates in contemporary glioblastoma surgery: results of an institutional protocol combining 5-aminolevulinic acid intraoperative fluorescence imaging and brain mapping. *Neurosurgery.* 2012;71(5): 927-935.
9. Stummer W, Novotny A, Stepp H, Goetz C, Bise K, Reulen HJ. Fluorescence-guided resection of glioblastoma multiforme by using 5-aminolevulinic acid-induced porphyrins: a prospective study in 52 consecutive patients. *J Neurosurg.* 2000;93(6):1003-1013.
10. Stummer W, Pichlmeier U, Meinel T, Wiestler OD, Zanella F, Reulen HJ. Fluorescence-guided surgery with 5-aminolevulinic acid for resection of malignant glioma: a randomised controlled multicentre phase III trial. *Lancet Oncol.* 2006; 7 (5):392-401.
11. Stummer W, Stocker S, Wagner S, et al. Intraoperative detection of malignant gliomas by 5-aminolevulinic acid-induced porphyrin fluorescence. *Neurosurgery.* 1998;42(3):518-525.
12. Valdés PA, Fan X, Ji S, Harris BT, Paulsen KD, Roberts DW. Estimation of brain deformation for volumetric image updating in protoporphyrin IX fluorescence-guided resection. *Stereotact Funct Neurosurg.* 2010;88(1):1-10.
13. Valdés PA, Leblond F, Kim A, et al. Quantitative fluorescence in intracranial tumor: implications for ALA-induced PpIX as an intraoperative biomarker. *J Neurosurg.* 2011;115(3):11-17.
14. Piccirillo SG, Dietz S, Madhu B, et al. Fluorescence-guided surgical sampling of glioblastoma identifies phenotypically distinct tumour-initiating cell populations in the tumour mass and margin. *Br J Cancer.* 2012;107(3):462-468.

15. Stummer W, Stepp H, Möller G, Ehrhardt A, Leonhard M, Reulen HJ. Technical principles for protoporphyrin-IX-fluorescence guided microsurgical resection of malignant glioma tissue. *Acta Neurochir (Wien).* 1998;140(10):995-1000.
16. Widhalm G, Wolfsberger S, Minchev G, et al. 5-Aminolevulinic acid is a promising marker for detection of anaplastic foci in diffusely infiltrating gliomas with nonsignificant contrast enhancement. *Cancer*. 2010;116(6):1545-1552.
17. Hefti M, von Campe G, Moschopulos M, Siegner A, Looser H, Landolt H. 5-aminolevulinic acid induced protoporphyrin IX fluorescence in high-grade glioma surgery: a one-year experience at a single institutuion. *Swiss Med Wkly.* 2008;138(11-12):180-185.
18. Idoate MA, Díez Valle R, Echeveste J, Tejada S. Pathological characterization of the glioblastoma border as shown during surgery using 5-aminolevulininic acid-induced fluorescence. *Neuropathology*. 2011;31(6):575-582.
19. Shapiro DE. The interpretation of diagnostic tests. *Stat Methods Med Res.* 1999; 8 (2):113-134.
20. Ando T, Kobayashi E, Liao H, et al. Precise comparison of protoporphyrin IX fluorescence spectra with pathological results for brain tumor tissue identification. *Brain Tumor Pathol.* 2011;28(1):43-51.
21. Utsuki S, Oka H, Sato S, et al. Histological examination of false positive tissue resection using 5-aminolevulinic acid-induced fluorescence guidance. *Neurol Med Chir (Tokyo).* 2007;47(5):210-214.
22. Lacroix M, Abi-Said D, Fourney DR, et al. A multivariate analysis of 416 patients with glioblastomamultiforme: prognosis, extent of resection, and survival. *J Neurosurg.* 2001;95(2):190-198.
23. McGirt MJ, Chaichana KL, Attenello FJ, et al. Extent of surgical resection is independently associated with survival in patients with hemispheric infiltrating low-grade gliomas. *Neurosurgery*. 2008;63(4):700-707.
24. Stummer W, Reulen HJ, Meinel T, et al. Extent of resection and survival in glioblastoma multiforme: identification of and adjustment for bias. *Neurosurgery*. 2008;62(3):564-576.
25. Stummer W, van den Bent MJ, Westphal M. Cytoreductive surgery of glioblastoma as the key to successful adjuvant therapies: new arguments in an old discussion. *Acta Neurochir (Wien).* 2011;153(6):1211-1218.
26. Kim A, Khurana M, Moriyama Y, Wilson BC. Quantification of in vivo fluorescence decoupled from the effects of tissue optical properties using fiber-optic spectroscopy measurements. *J Biomed Opt.* 2010;15(6):067006.
27. Ramanujam N. Fluorescence spectroscopy of neoplastic and non-neoplastic tissues. *Neoplasia*. 2000;2(1-2):89-117.
28. Richards-Kortum R, Sevick-Muraca E. Quantitative optical spectroscopy for tissue diagnosis. *Annu Rev Phys Chem.* 1996;47:555-606.
29. Sokolov K, Follen M, Richards-Kortum R. Optical spectroscopy for detection of neoplasia. *Curr Opin Chem Biol.* 2002;6(5):651-658.
30. Haj-Hosseini N, Richter J, Andersson-Engels S, Wårdell K. Optical touch pointer for fluorescence guided glioblastoma resection using 5-aminolevulinic acid. *Lasers Surg Med.* 2010;42(1):9-14.
31. Ishihara R, Katayama Y, Watanabe T, Yoshino A, Fukushima T, Sakatani K. Quantitative spectroscopic analysis of 5-aminolevulinic acid-induced protoporphyrin IX fluorescence intensity in diffusely infiltrating astrocytomas. *Neurol Med Chir (Tokyo).* 2007;47(2):53-57.
32. Utsuki S, Oka H, Miyajima Y, Shimizu S, Suzuki S, Fujii K. Auditory alert system for fluorescence-guided resection of gliomas. *Neurol Med Chir (Tokyo).* 2008;48 (2):95-98.
33. Utsuki S, Oka H, Sato S, et al. Possibility of using laser spectroscopy for the intraoperative detection of nonfluorescing brain tumors and the boundaries of brain tumor infiltrates. Technical note. *J Neurosurg.* 2006;104(4):618-620.

COMMENTS

It is very helpful to remember that GBM is a diffuse tumor. It does not have a real border, and it blends with the parenchyma. MRI T1Gd volume is a good surrogate for solid tumor mass, and its clinical utility has been proved, but it should not be considered as a perfect measurement of solid tumor, nor should it be confused with the whole tumor. The authors elegantly validated by neuropathology and objective measurement with spectrometry how the different qualities of fluorescence reflect a gradient in tumor invasion. The differences in "weak fluorescence," "near" and "distant" suggest a high degree of invasion just around the T1Gd, similar to what has been suggested in previous works with 5-ALA[1] and PET imaging.[2]

This important work confirms that the neurosurgeon using 5-ALA can identify both areas of solid tumor and areas where tumor blends with the tissue. It is of paramount importance to understand this technique to make proper use of it, and this article should be compulsory reading to all using 5-ALA.

Ricardo Díez Valle
Navarra, Spain

1. Aldave G, Tejada S, Pay E, et al. Prognostic value of residual fluorescent tissue in glioblastoma patients after gross total resection in 5-aminolevulinic acid-guided surgery. *Neurosurgery*. 2013;72(6):915-20; discussion 920-921.
2. Arbizu J, Tejada S, Marti-Climent JM, et al. Quantitative volumetric analysis of gliomas with sequential MRI and (11)C-methionine PET assessment: Patterns of integration in therapy planning. *Eur J Nucl Med Mol Imaging.* 2012.

This study attempts to quantify a phenomenon observed early in the development of fluorescence guided glioma resection with 5-aminolevulinic acid (ALA): there are degrees of fluorescence brightness that represent different densities of tumor involvement. Strong fluorescence indicates tissue with more than 80% tumor cells, whereas weakly fluorescent areas have less than 50% tumor cell density on average.

The findings that strong, red fluorescence visualized with the operating microscope has a positive predictive value (PPV) of 100% for tumor, and weak, pink fluorescence has PPV of 92%, are consistent with the pooled results from other studies.[1]

Further, macroscopic fluorescence does not indicate all of the tissue containing tumor. The negative predictive value (NPV) of non-fluorescing tumor is only 24%. Spectroscopic analysis indicates that these tumor containing regions do fluoresce compared to uninvolved brain, and that the brightness of fluorescence correlates with tumor cell density, but the fluorescence is not evident under the operating microscope. These regions also have a high proportion of normal cells. The addition of spectroscopy therefore reduces specificity but increases sensitivity and NPV.

Intriguingly, the results suggest that complete resection of fluorescence may provide a significant cytoreductive advantage over and above complete resection of enhancement, as only 15/23 cases (14/42 sampled regions) with residual fluorescence demonstrated residual enhancement on post operative MRI. Recent evidence indicates that this cytoreduction, measured by complete resection of fluorescence, confers a survival benefit over complete resection of enhancement (Aldave, Tejada, Pay et al 2013) but further studies are needed.

This study confirms what surgeons using ALA have noted, that the use of fluorescence guidance frees the surgeon's attention from the question of "is this tumor" and allows greater consideration of whether the tissue is safe to resect, given the local anatomy. The challenge for the future remains to develop techniques to control the tumor that is neither macroscopically fluorescent nor safely resectable.

Michael J. Colditz
Rosalind L. Jeffree
Brisbane, Australia

1. Colditz MJ, Jeffree RL. Aminolevulinic acid (ALA)-protoporphyrin IX fluorescence guided tumor resection. Part 1: Clinical, radiological and pathological studies. *J Clin Neurosci.* 2012;19(11):1471-1474.

The authors provide a thoughtful analysis of 33 patients with high-grade gliomas who received 5-aminolevulinic acid (5-ALA) before resection. Their findings support our understanding of this agent as a relatively reliable biomarker for glioma infiltration, even when visible signal is weak. Any neuropathological assessment of tumor vs nontumor has inherent limitations, however, which is why there is a continued need for analysis of the "cellular" specificity of 5-ALA for human gliomas.

Nader Sanai
Phoenix, Arizona

The Danube

The Danube is the European Union's longest and the continent's second longest river. Once a long-standing frontier of the Roman Empire, the river passes through or touches the borders of ten countries. The Danube is a source of drinking water for about twenty million people. In Germany, almost 30% of the water for the area between Stuttgart, Bad Mergentheim, Aalen and Alb-Donau comes from purified water of the Danube. In Austria and Hungary, most find it too difficult to clean the water because of extensive pollution; only parts of Romania where the water is cleaner still obtain drinking water from the Danube on a regular basis.